Journal of Neural Engineering

Controlled local release of PPARγ agonists from biomaterials to treat peripheral nerve injury

To cite this article before publication: Melissa Lucy Doreen Rayner *et al* 2020 *J. Neural Eng.* in press https://doi.org/10.1088/1741-2552/aba7cc

Controlled local release of PPARγ agonists from biomaterials to treat peripheral nerve injury

MLD Rayner [1, 2, 3], A Grillo [1, 3], GR Williams [2], E Tawfik [2, 4], T Zhang [2], C Volitaki [2], DQM Craig [2], J Healy [2, 3] and JB Phillips [1, 2, 3].

[1] Biomaterials & Tissue Engineering, UCL Eastman Dental Institute, UCL, London, UK.
[2] UCL School of Pharmacy, UCL, London, UK.
[3] UCL Centre for Nerve Engineering, London, UK.
[4]National Center for Pharmaceutical Technology, King Abdulaziz City for Science and Technology, Riyadh, Kingdom of Saudi Arabia.

Abstract

Objective: Poor clinical outcomes following peripheral nerve injury (PNI) are partly attributable to the limited rate of neuronal regeneration. Despite numerous potential drug candidates demonstrating positive effects on nerve regeneration rate in preclinical models, no drugs are routinely used to improve restoration of function in clinical practice. A key challenge associated with clinical adoption of drug treatments in nerve injured patients is the requirement for sustained administration of doses associated with undesirable systemic side-effects. Local controlled-release drug delivery systems could potentially address this challenge, particularly through the use of biomaterials that can be implanted at the repair site during the microsurgical repair procedure.

Approach: In order to test this concept, this study used various biomaterials to deliver ibuprofen sodium or sulindac sulfide locally in a controlled manner in a rat sciatic nerve injury model. Following characterisation of release parameters *in vitro*, ethylene vinyl acetate (EVA) tubes or polylactic-co-glycolic acid (PLGA) wraps, loaded with ibuprofen sodium or sulindac sulfide, were placed around directly-repaired nerve transection or nerve crush injuries in rats.

Main results: Ibuprofen sodium, but not sulindac sulfide caused an increase in neurites in distal nerve segments and improvements in functional recovery in comparison to controls with no drug treatment.

Significance: This study showed for the first time that local delivery of ibuprofen sodium using biomaterials improves neurite growth and functional recovery following PNI and provides the basis for future development of drug-loaded biomaterials suitable for clinical translation.

Keywords

Nerve regeneration; Non-steroidal anti-inflammatory drugs (NSAIDs); Local drug delivery; Biomaterials; Peroxisome proliferator-activated receptor gamma (PPARγ); Peripheral nerve injury (PNI).

Acknowledgements

This research was made possible through the funding of the EPSRC (Grant EP/L01646X).

Declarations of interest: none.

Introduction

Peripheral nerve injury (PNI) is associated with substantial socioeconomic impact as the resulting disability can be debilitating, significantly affecting the patient's quality of life *(1-4)*. Treatments mainly employ microsurgical interventions although additional therapeutics that can be administered following PNI have emerged such as cell therapies, proteins, platelet-rich plasma and gene therapy *(5-8)*. There are currently no drug therapies that are routinely used to promote regeneration in nerve injured patients, despite various candidate drugs showing benefit in preclinical models *(9, 10)*. One drug which has been shown to improve regeneration when administered systemically to rats following PNI is ibuprofen, a non-steroidal anti-inflammatory drug (NSAID) which is likely to accelerate neurite elongation as an agonist of peroxisome proliferator-activated receptor gamma (PPARγ) *(11, 12)*. Another NSAID with PPARγ agonist activity is sulindac sulfide, which has not been tested for use in nerve repair previously.

Pharmaceutical challenges that have prevented translation of drug therapies such as ibuprofen from preclinical to human usage in PNI include the provision of adequate drug dose and duration while reducing unwanted side effects associated with systemic administration *(13)*. Long term oral treatment in particular can lead to side effects and also problems with patient compliance *(14)*. Delivering drugs locally using biomaterials provides a potential new approach to address these challenges, therefore this study aimed to investigate local delivery of both ibuprofen sodium and sulindac sulfide.

Biomaterials suitable for implantation at the site of nerve injury include synthetic polymers and natural materials that would biodegrade over time, with the potential to provide controlled-release of drug *(4, 15)*. Controlled-release systems using degradable and non-degradable biomaterials to deliver drugs have demonstrated effectiveness in other indications *(15-17)* and can be tested for application in a neural environment. Most drug-release materials are relatively short-acting, however for nerve injury there is likely to be benefit in releasing pro-regenerative drugs over a sustained period of weeks to maximize benefit throughout the

regeneration period. In order to explore various approaches for the local delivery of ibuprofen sodium and sulindac sulfide, a range of materials including ethylene vinyl acetate (EVA), polycaprolactone (PCL), polylactic-co-glycolic acid (PLGA) and mesoporous silica nanoparticles (MSN) were selected for use in this study.

As a further innovation, these drug-loaded polymers have been prepared both as sheets using solvent casting and as nanofibres using electrospinning. This latter approach involves the application of a voltage to an extruded polymer solution so as to result in the generation of fibres, which can then be used for numerous delivery and biomaterial applications. Here we explore the use of these fibres as a drug-loaded sheath to provide both physical support and prolonged release of the therapeutic agents.

EVA is a non-degradable polymer approved for use in a range of clinical applications to deliver drugs such as hormonal contraception, pilocarpine for glaucoma and buprenorphine for opioid addiction *(16, 18)*. PCL is a biocompatible aliphatic polyester used clinically for hormonal contraceptive implants and it has been extensively investigated as a nerve conduit for PNI repair *(19, 20)*. Currently, a Phase I clinical trial is recruiting participants to evaluate the use of PCL nerve conduits as a therapy in sensory digital nerve surgery *(21)*. An attempt at ibuprofen loading into PCL has been reported in relation to development of nerve conduits although the effects on neuronal regeneration were not tested *in vitro* or *in vivo (22).* PLGA has been used to deliver growth factors, hormones and drugs in experimental PNI treatment *(23)*. MSNs are versatile drug-delivery materials *(24)* and previous studies using ibuprofen have shown a high loading content of the poorly soluble drug and a release rate of 96.3% *(25)*, making them another promising material for investigation in PNI.

The overall goal of this study was to test whether NSAIDs could be delivered locally to improve regeneration following PNI, thus potentially overcoming the limitations associated with systemic administration. In the first instance, a range of drug/material combinations were developed and tested *in vitro* to establish stability and drug-release parameters. Controlled-release formulations of NSAIDs in polymeric sheaths of EVA and PLGA were then positioned

around a nerve transection and crush injury respectively in a rat PNI model, increasing neurite growth and supporting the hypothesis that locally delivered NSAIDs might be of benefit.

Material and methods

All materials were supplied by Sigma-Aldrich unless otherwise stated.

Drug loading into biomaterials

Drug embedded EVA membranes were manufactured by dissolving 2 g EVA co-polymer beads and 1 %, 2 % or 4 % (w/v) ibuprofen sodium in 20 mL chloroform. Once the drug and the polymer had fully dispersed, the solution was added to a rectangular 83 mm x 63 mm glass mould and dried at room temperature for 24 h. The membrane was then cut into 5 mm x 12 mm x 0.5 mm flat sheets for characterisation and implantation studies. EVA sheets with no embedded drug were manufactured using the same procedure and used as control samples. EVA membranes were manufactured into tubular-shaped constructs for implantation by wrapping the EVA sheet around a 19G needle and applying ~50 µl of chloroform to fuse the two edges together. The tubes were dried at room temperature and removed from the needle furnishing a tube with dimensions 5 mm x 12 mm and 1.5 mm inner diameter. This method of fabrication was selected as it has been used previously for pranoprofen delivery *(26)*.

Drug embedded PCL membranes were manufactured by dissolving 100 mg ibuprofen sodium in 5 mL chloroform then adding 5 g PCL beads to the solution and stirring for 18h at room temperature. The homogenous polymer solution was poured into a circular Teflon mould (Ø 77 mm) and dried for 2-3 h at room temperature to allow the solvent to evaporate. Once the solvent was removed the membrane was cut into smaller sheets (7 mm x 12 mm x 0.4 mm) for characterisation. PCL membranes without drug were prepared using the same procedure and used as control samples.

100 mg of mesoporous silica nanoparticles (MSN) (kindly donated by Ahmed El-Fiqi, UCL Eastman Dental Institute) (24) were dispersed in 10 mL ibuprofen sodium solution (2% w/v prepared in distilled water) and incubated for 6 hours at 37 °C to allow drug loading. The

resulting solution was centrifuged at 400 g for 5 minutes to obtain a pellet of MSN. They were then left to dry at 37 °C overnight. During this time the MSN aggregated and formed clumps so the pellet was ground to re-obtain a powder. Drug loading into the MSN was determined by measuring the quantity of ibuprofen remaining in the stock solution using UV-Vis spectrophotometry (Unicam UV500).

A PCL membrane with ibuprofen-loaded MSN was made by dispersing the MSN in 5 mL chloroform (1% or 2% of ibuprofen-loaded MSN, which corresponded to 50 mg and 100 mg of MSN, respectively). 500 mg of PCL beads were added to this solution and the mixture was stirred at room temperature for 18h. The MSN loaded PCL was manufactured using the same method.

Electrospinning of Poly (lactic-co-glycolic acid) (PLGA)

Poly (lactic-co-glycolic acid) (PLGA) (Corbion Purac with molecular weight (MW) of 96,000 Grade: PURASORB PDLG 7507 ratio 75:25) nanofibres were fabricated by electrospinning using a Spraybase® electrospinning instrument (Spraybase®). The PLGA 17.5% w/v was dissolved in dichloromethane (DCM) and stirred gently for 45 min. Then 2.5% w/v ibuprofen sodium or 1% w/v sulindac sulfide was added and stirred for another 45 min to achieve a drug to polymer ratio of 1:7, or 1:17 respectively. These ratios were obtained after optimising the fabrication of both drug-loaded fibrous systems, which ensured the production of more uniform and reproducible fibres with high drug loading profiles. The solution was loaded into a 10 mL syringe to be ejected through a 0.7 mm diameter needle. The flow rate and voltage used to stabilise the jet were 1 mL/h and 10-11 kV, respectively. The fibres were collected on aluminium foil at a distance of 12.5 cm. Similar parameters were used to prepare blank fibres with no drug embedded. The drug encapsulation efficiency and drug loading was determined by dissolving the fibres in 20 mL of acetonitrile for 4 h. The resulting solutions were analysed using UV-Vis spectroscopy.

Material characterization

Scanning electron microscopy (SEM)

The morphology and particle size of the polymeric samples were characterized using SEM (Philips XL30 FEG or FEI Quanta 200F) at 5 kV. Samples were mounted onto metal specimen stubs, using double-sided adhesive tape, vacuum coated with a platinum film and then viewed and imaged. The particle size and porous structure of MSN were characterised using TEM (Philips CM12) operated at 80 kV.

Drug release

Drug release was determined by incubating the material in 1 mL distilled water at 37 °C. 1 mL aliquots were collected at fixed time points (1 h, 2 h, 3 h, 4 h and then every 24 h) and replaced with 1 mL of fresh distilled water. The solution collected was analysed with a UV-Vis spectrophotometer (Unicam UV500) at a wavelength of 263 nm. Initially samples were mildly agitated however this caused no difference in the release so was not continued.

X-ray diffraction (XRD)

XRD spectra were acquired using Rigaki Miniflex 600 diffractometer, supplied with Cu Kα radiation (λ = 1.5418 Å) at 40 kV and 15 mA.

Differential scanning calorimetry (DSC)

DSC was conducted by charging a Tzero pan with ≤ 5 mg of material and analysing this with a Q2000 calorimeter (TA Instruments). A temperature ramp of 10 ºC/min was used over the range of 0-170 ºC.

Thermogravimetric analysis (TGA)

5 mg of sample was loaded into Al TGA pans. TGA was performed on a TA Discovery instrument, with the sample heated at a rate of 20 ºC/min to a maximum of 400 ºC. The nitrogen purge was set at 25 mL/min and balance purge flow of 10 mL/min.

The mechanical properties of a scaffold vary according to fabrication method, thickness, and many other factors. The literature suggests that the tensile strength of similar systems is in

the order of <10 MPa. For instance, EVA films have been reported to have strengths lying in the range 2 – 5 MPa *(27)*, PCL membranes 2-14 MPa *(28)* and electrospun PLGA fibers 0.3 – 1.5 MPa *(29)*.

Surgical nerve injury models

All surgical procedures were performed in accordance with the UK Animals (Scientific Procedures) Act (1986), the European Communities Council Directives (2010/63/EU) and approved by the UCL Animal Welfare and Ethics Review Board. Adult male Wister rats (250-300 g) (Charles River) were deeply anaesthetised by inhalation of isoflurane, and the left sciatic nerve was exposed at mid-thigh level then subjected to either a transection or a crush injury. A transection injury with a primary repair was conducted by making a cut through the entire nerve (1.5 cm distal of the femur) and the proximal and distal stumps were re-connected using two 10/0 epineurial sutures, one on each side of the nerve at each stump. EVA tubes pre-loaded with vehicle control or drug treatment were placed around the injury site like a cuff by threading a nerve stump through the tube between transection and repair, then sliding the tube over the repair after suturing. The crush injury was achieved by applying a consistent pressure with a pair of sterile TAAB tweezers type 4 closed fully on the same point of the nerve (1.5 cm distal of the femur) for 15 s. This was repeated twice more in the same location with the tweezers positioned perpendicular to the nerve and rotated through 45° between each crush application *(30)*. A 10/0 epineurial suture (Ethicon) was used to mark the location of the crush. The ibuprofen sodium- or sulindac sulfide–loaded PLGA was wrapped around the injury site once as a single layered cuff.

The overlying muscle layers were closed using two 4/0 sutures (Ethicon) and the skin was closed using stainless steel wound clips. Animals were allowed to recover and were maintained for 21 or 28 days then culled using CO_2 asphyxiation and the repaired nerves were excised under an operating microscope and immersion-fixed in 4% (w/v) paraformaldehyde in PBS at 4 ºC. The gastrocnemius muscles on both the repaired and contralateral side were separated from the soleus muscle and stored in 4% PFA on ice and weighed immediately.

Electrophysiology

After 21 – 28 days animals were anaesthetised using isoflurane and nerve function was assessed using electrophysiology (Sapphire 4ME system) by comparing the repaired nerve to the contralateral undamaged nerve in each animal. Electrodes (Natus) were attached to the animal; a grounding electrode was placed onto the tail of the animal and a reference electrode was placed above the hip bone. A stimulating electrode (Neurosign Bipolar Probe 2 × 100 mm × 0.75 mm electrode) was placed against the proximal nerve 2 mm above the injury site and a monopolar recording needle (Ambu® Neuroline concentric) was placed into the gastrocnemius muscle. The distance between the stimulating and recording electrodes was standardised. The nerve was stimulated using a bipolar stimulation constant voltage configuration and the muscle response recorded. The stimulation threshold was determined by increasing the stimulus amplitude in 0.1 V steps (200 μs pulse), until both a supramaximal, stimulus-correlated compound muscle action potential (CMAP) was recorded and a significant twitch of the animal's hind paw could be seen. The CMAP amplitude (mV) was measured from baseline to the greatest peak and the latency was measured from the time of stimulus to the first deviation from the baseline. CMAPs were recorded in triplicate for both the injured nerve and contralateral control nerve in each animal.

Von Frey sensory assessment

The animals were placed on a grid and von Frey filaments (0.008 g - 300 g) were applied through the underside of the grid to stimulate the centre of the animal's hind paws. A response was determined by the retraction of the animal's paw following the filament stimulus. The threshold response was recorded by decreasing the stimulus until no response was detected.

Static sciatic index (SSI)

The animal's hind paws were imaged and the toe spread factor (TSF), between the 1st and 5th toe, and the intermediary toe spread factor (ITSF), between the 2nd and 4th toe, were measured and equation 1 was used to calculate SSI *(31)*.

Equation 1: $SSI = (108.44 \times TSF) + (31.85 \times ITSF) - 5.49$

$TSF = TS_{control} - TS_{injury}$, $ITSF = ITS_{control} - ITS_{injury}$

Cryo-sectioning

Following fixation the nerve samples were incubated in 30% sucrose overnight and underwent subsequent snap freezing in 1:1 FSC 22 Frozen Section Media (Leica) and 30% sucrose. Transverse sections (10 µm) were prepared from the proximal and distal stumps 5 mm from the injury site, using a cryostat (Leica CM1860). The sections were adhered to glass slides (Superfrost™ Plus, Thermo Fisher Scientific) for histological analysis.

Immunohistochemistry

Nerve sections were washed in immunostaining buffer (PBS together with 0.2% Triton-X100, 0.002% sodium azide and 0.25% Bovine Serum Albumin before the addition of serum (Dako) to block non-specific binding (1:20 dilution). After 30 mins the blocking serum was removed and sections were incubated with neurofilament-H (Eurogentec, 1:1000) or RECA-1 (Millipore, 1:100) primary antibody diluted in immunostaining buffer overnight at 4 ºC. The sections were washed with immunostaining buffer before addition of the Dylight 549 or 488 secondary antibody (Vector Laboratories, 1:400) and incubation at room temperature for 45 mins. Sections underwent a final wash with immunostaining buffer before mounting with Vectashield Hardset mounting medium with DAPI (Vector Laboratories).

Image analysis and quantification

Tile scans were used to capture high-magnification (x20) micrographs from the entire nerve cross-section using a Zeiss LSM 710 confocal microscope and images were analysed using

Volocity™ 6.4 (PerkinElmer) running automated image analysis protocols to determine the number of neurofilament-immunoreactive neurites in each transverse nerve section. Blood vessel analysis was conducted from entire nerve sections using fluorescence microscopy (Zeiss Axiolab A1, Axiocam Cm1) and blood vessel diameter was measured using ImageJ software *(32)*.

Other segments of nerve samples were dissected and transferred to 3 % glutaraldehyde (Agar Scientific) in 0.1 M cacodylate buffer. The samples were then post-fixed in 1% (w/v) osmium tetroxide in PBS, dehydrated using a graded series of ethanol incubations, flat-embedded in TAAB embedding resin and polymerized at 60 °C for 48 h. Semi-thin sections of 0.5 µm were cut using a diamond knife on an Ultracut E microtome (Leica) then dried onto microscope slides. They were then stained with 1% (w/v) toluidine blue with added 5% (w/v) sodium borate and imaged using light microscopy with oil immersion using a x5 and x100 lens.

Residual drug in EVA constructs

At the end of the *in vivo* release experiments the residual drug content of the conduits was measured. Briefly, the conduits were dissolved in 5 mL of chloroform and once the polymer had completely dissolved it was separated from the drug by adding 3 mL of distilled water. The solution was incubated at room temperature for 24 h in order to allow the phases to separate. The amount of ibuprofen was determined using a UV-Vis spectrophotometer at a wavelength of 263 nm.

Statistical analysis

Normality tests were conducted on all data to determine appropriate statistical tests, and one-way analysis of variance (ANOVA) or t-tests were performed, as data followed a normal distribution. A one-way ANOVA was followed by a Tukey or Dunnett post hoc test. For all tests, *p<0.05, **p<0.01, ***p<0.001 and ****p<0.0001 were considered to be significant.

Results

Characterisation of materials

Ethylene vinyl acetate (EVA)

Scanning electron micrographs indicated that pore size of the fabricated membranes changed as a result of drug loading, with pores ~5 μm in the control and ~25 μm in the ibuprofen-loaded material (Figure 1 (a-d)). Crystals of drug were visible within the pores (Figure 1 (c), (d)). EVA tubes with and without ibuprofen sodium were also imaged by SEM following cryogenic fracture in liquid nitrogen (Figure 1 (e-h)). Tubes of the required diameter could be formed by overlapping and fusing the edges of the membrane (Figure 1 (e), (g)).

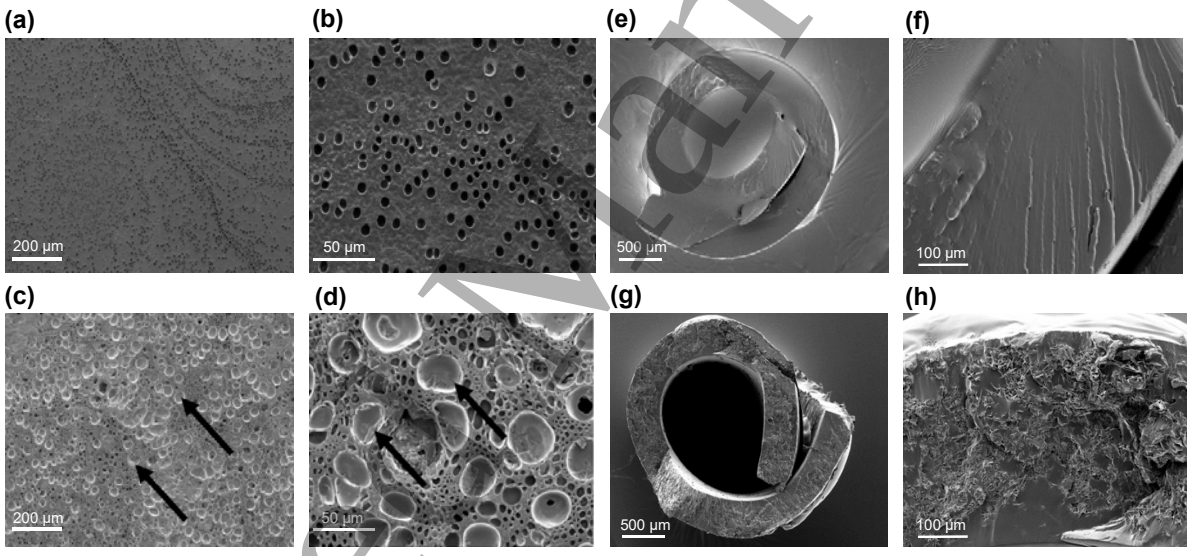

Figure 1: SEM images of blank and ibuprofen-loaded EVA membranes and tubes. The images were taken following cryogenic fracture of blank EVA membranes (a, b), ibuprofen-loaded EVA membranes (c, d), blank EVA tubes (e, f) and ibuprofen-loaded EVA tubes (g, h). Pores in the ibuprofen-loaded EVA membranes indicated with black arrows.

X-ray diffraction (XRD) data revealed sharp Bragg reflections in the case of the initial ibuprofen sodium material, showing it to be a crystalline material (Figure 2 (a)). A comparison with the literature pattern (CSD entry 2015083) confirmed the raw material to comprise sodium ibuprofen dihydrate (Figure 2 (a)). EVA itself is clearly amorphous, showing a typical halo feature in its XRD pattern. The ibuprofen-loaded EVA membrane combines the features of the two raw materials. There is an amorphous halo present, superimposed upon which are weak

reflections at the same position as the ibuprofen starting material. There is thus some crystalline sodium ibuprofen dihydrate present in the drug-loaded membrane, which suggests that the drying process was relatively slow.

Thermogravimetric analysis (TGA) measures the mass of the sample as the temperature increases over time. The ibuprofen sodium starting material shows mass loss of ca. 13.5% between room temperature and 100 ºC (Figure 2 (b)). This agrees well with the theoretical mass loss of 13.6% upon going from the dihydrate to the anhydrous form of sodium ibuprofen. There is some mass loss below 150 ºC in the case of ibuprofen-loaded EVA, which could also be due to the inclusion of water. Both the EVA and drug loaded membrane experienced mass loss at ~ 300 ℃ which represents the degradation of the polymer (Figure 2 (b)).

Differential scanning calorimetry (DSC) results (Figure 2 (c)) show water loss from ibuprofen sodium dihydrate (peak max: 102.9 ºC), and also for the drug-loaded EVA membrane (100.3 ºC). A distinct baseline shift can be seen for EVA and ibuprofen-loaded EVA, between 35 and 40 ºC (onsets are 36.6 and 36.1 ºC respectively). This is the glass transition temperature (Tg) and confirms the presence of an amorphous phase. The fact that the Tg of the drug-loaded membrane is very close to that of raw EVA could be taken to indicate that the membrane comprises amorphous EVA with crystalline ibuprofen particles within it.

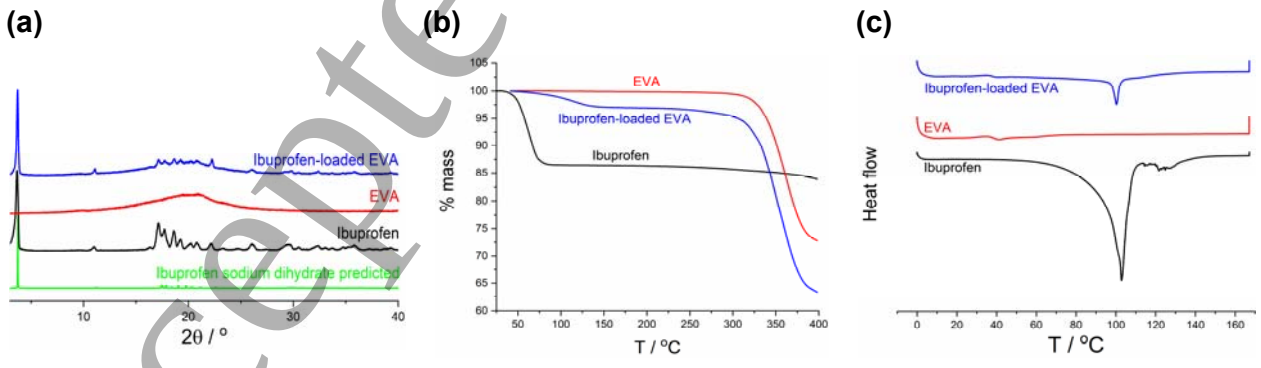

Figure 2: (a) XRD, (b) TGA and (c) DSC data (exo up) for blank and ibuprofen-loaded EVA.

Drug release

In vitro drug release from ibuprofen-loaded EVA membranes and tubes was rapid in the first 4 h and then plateaued at 24 h. Over 30% of the drug was released in the first 4 h with a 4% drug load while only 12% was released with the 0.5% drug load over the same time. The 2% drug load achieved the highest release over 10 days at 92%, whereas, for 0.5%, 1% and 4 % drug loading, 84%, 65% and 67% drug release respectively were observed (Figure 3 (a)). Therefore, the 2% drug load concentration was taken forward for further investigation. Furthermore, under the conditions used for drug release experiments, it was found that a tube geometry slowed the release profile in the first few days compared to flat sheets, with the release plateauing at 5 days (Figure 3 (b)).

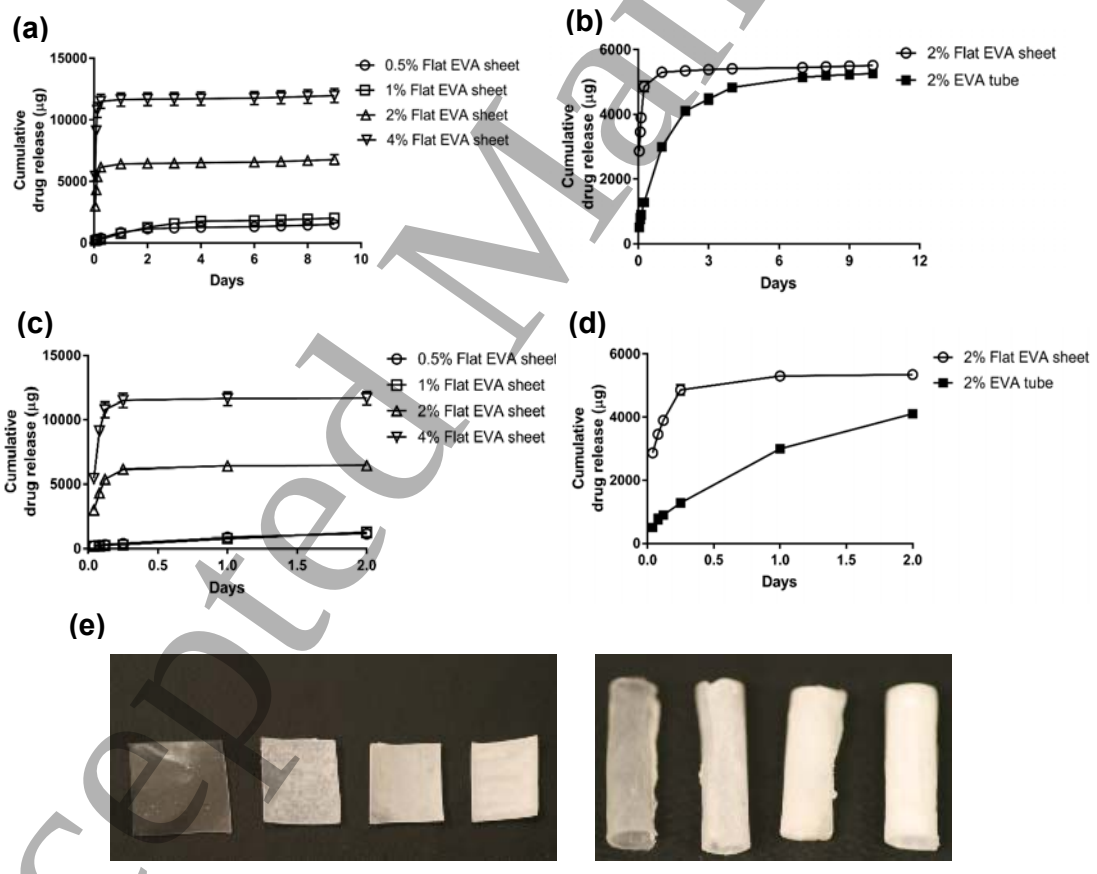

Figure 3: Drug release from ibuprofen-loaded EVA. Comparison of increasing concentration drug loads 0.5%, 1%, 2% and 4% ibuprofen sodium loading into flat sheet membranes (a) and comparison of release from an EVA membrane and tube loaded with 2% ibuprofen sodium (b) with sub plots beneath to show the initial burst of release in the first 2 days (c, d). Manufactured EVA sheets and tubes with 0.5%, 1%, 2% and 4% ibuprofen loading (e). N=3, mean ± SEM.

Polycaprolactone (PCL)

The composition and morphology of the PCL membranes either blank or loaded with 2% ibuprofen sodium or ibuprofen-loaded MSN were analysed using SEM (Figure 4). No pores could be seen and small crystals of drug were deposited over the surface of the membrane (Figure 4 (b)). Drug loading was random and not homogenous, however, the homogeneity improved with MSN loading *c.f.* pure drug (Figure 4 (c)) and less drug was deposited on the surface.

Drug release

In vitro drug release from ibuprofen-loaded and MSN-loaded PCL membranes was rapid in the first 4 h and then plateaued and remained constant after 24 h. The release of ibuprofen was slower when loaded into MSN before embedding into PCL (Figure 4 (e)). After ~9 days ~80% of drug was released in the ibuprofen loaded PCL, whereas, only ~20% of ibuprofen was released from the MSN-loaded PCL. It is hypothesised that embedding the drug into MSN and PCL produces a dual release mechanism which improves the controlled release of ibuprofen. However, when using a similar loading of 1-2% of drug only or drug-loaded MSN into the PCL the latter resulted in less total drug within the material. This could potentially be due to loss of drug during the additional preparation stages for MSN-loaded PCL. Both of these drug delivery platforms needed further optimisation to obtain efficient drug release and so were not explored further in this study.

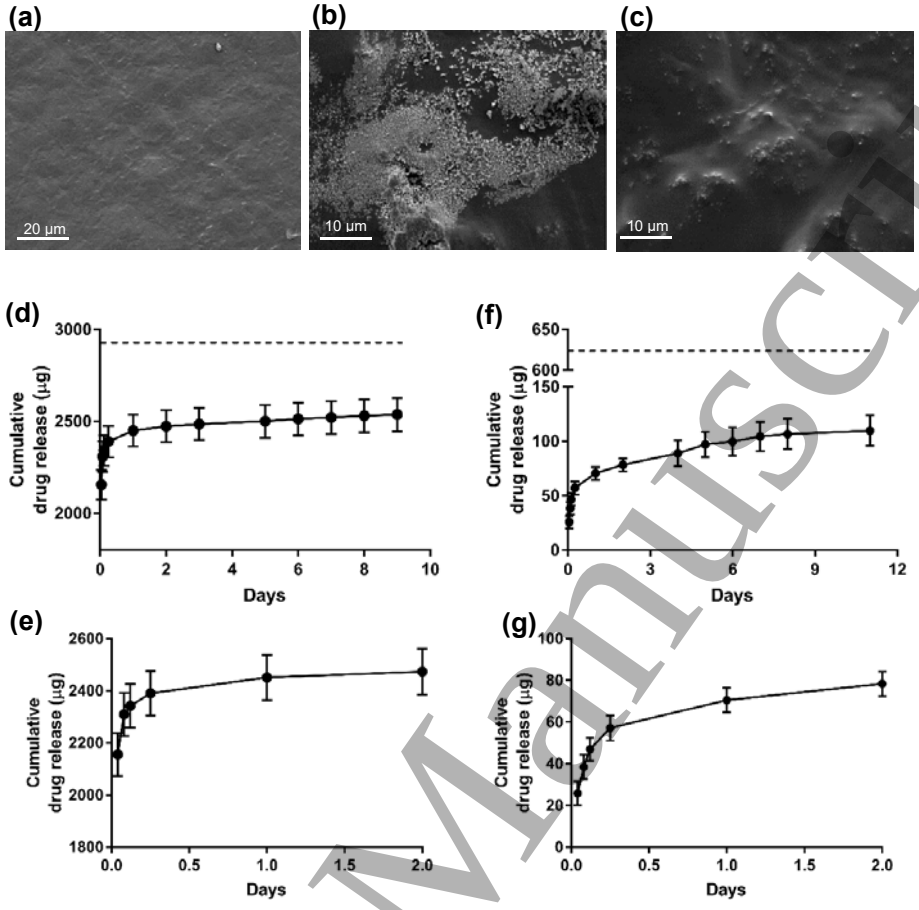

Figure 4: SEM images of blank, ibuprofen-loaded PCL membranes and ibuprofen-loaded MSN embedded in PCL. Blank PCL membranes (a) ibuprofen-loaded PCL membranes (b) and ibuprofen-loaded MSN embedded in PCL (c). Drug release from ibuprofen-loaded PCL (d) and ibuprofen-loaded MSN embedded in PCL (f). The initial drug load is shown by the dotted line. Sub plots to show the initial drug release in the first 2 days for ibuprofen-loaded PCL (e) and ibuprofen-loaded MSN embedded in PCL (g). N=3, mean ± SEM.

Poly (lactic-co-glycolic) acid (PLGA)

The composition and morphology of the electrospun PLGA nanofibres with and without ibuprofen sodium or sulindac sulfide were analysed using SEM (Figure 5). The nanofibres with a 1:7 ratio of drug to polymer were smooth and randomly aligned with an average diameter of 0.92 µm.

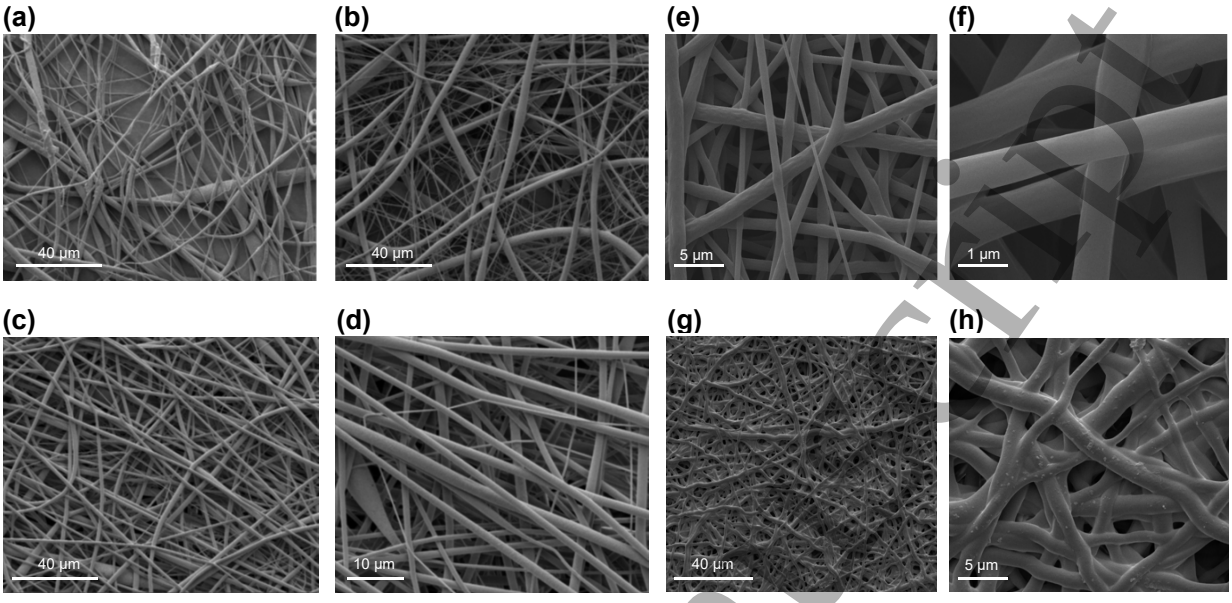

Figure 5: SEM images of blank and ibuprofen sodium or sulindac sulfide-loaded electrospun PLGA nanofibres. Blank PLGA nanofibres (a, b) and ibuprofen-loaded PLGA nanofibres (c, d). The nanofibres presented different surface appearances under different storage conditions; (e, g) at 4 ºC and (f, h) at 27 ºC for 7 days.

XRD analysis (Figure 6 (a)) showed that the initial crystalline form of ibuprofen sodium is not carried through into the electrospun fibres. The sharp Bragg reflections of the drug are not seen with the ibuprofen-loaded PLGA fibres. This demonstrates that the resulting fibres are amorphous and the drug molecules are randomly dispersed within the polymer matrix. The distinctive mass loss seen in the TGA for ibuprofen sodium between room temperature and 100 ºC (corresponding to water loss from the dihydrate form of the sodium salt) is not visible for the fibres (Figure 6 (b)). This is replaced by a more gradual mass loss from occluded water, which is complete by ca. 175 ºC. In DSC, the PLGA raw material shows a glass transition (onset: 53.9 ºC) with is overlaid with a relaxation endotherm. Both the relaxation endotherm and the ibuprofen sodium dehydration event at ca. 100 ºC do not arise with the fibres, which show only a poorly defined Tg event with onset at ca. 44 ºC. This change in Tg indicates plasticisation of the polymer chains by the incorporated ibuprofen sodium (Figure 6 (c)). This is consistent with the formation of an amorphous solid dispersion in the form of a solid solution.

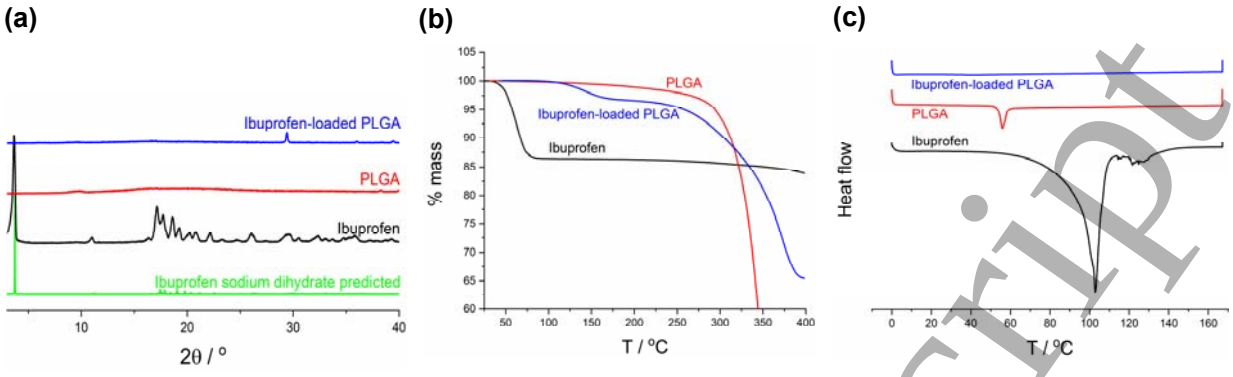

Figure 6: (a) XRD, (b) TGA and (c) DSC data (exo up) for blank and ibuprofen-loaded PLGA nanofibres.

Drug release

In vitro drug release from ibuprofen sodium and sulindac sulfide-loaded PLGA nanofibres was measured every hour for 6 h, then every 24 h for 7 days and at 14 and 21 days. The ibuprofen-loaded PLGA nanofibres demonstrated a rapid release with ~88 % of the drug released within 7 days (Figure 7 (a)). The sulindac sulfide-loaded PLGA nanofibres demonstrated first order release, with 100% of the drug released within ~18 days (Figure 7 (b)).

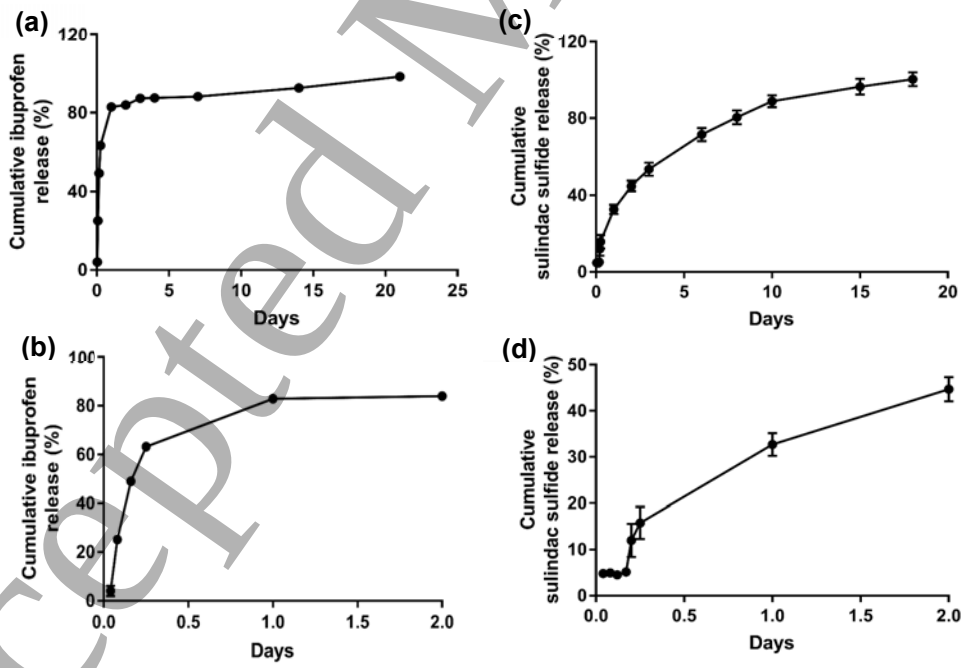

Figure 7: Drug release from ibuprofen sodium and sulindac sulfide-loaded electrospun PLGA nanofibres. Ibuprofen-loaded nanofibres (a) and sulindac sulfide-loaded nanofibres (c). Sub plots to show the initial drug release from ibuprofen-loaded nanofibres (b) and sulindac sulfide-loaded nanofibers in the first 2 days (d). N=3, mean ± SEM.

Effect of drug-loaded materials on nerve regeneration

Having established various approaches for incorporating ibuprofen sodium and sulindac sulfide into materials that might be useful in a nerve injury scenario, two selected formulations were taken forwards to test the concept *in vivo* using a rat model. The first selected formulation was ibuprofen-loaded EVA which provided a robust a reproducible method for testing the local delivery of ibuprofen sodium to a nerve transection injury. EVA tubes were threaded onto transected nerves at the time of repair in order to test the concept of local release of ibuprofen sodium from a biomaterial during the days following injury. The dose of ibuprofen delivered was based on an effective dose established in our previous study, used *in vitro* and delivered *in vivo,* using osmotic pumps *(12)*. The outcome measure of interest was a histological analysis of the number of neurites that had regrown across the transection site and entered the distal stump at 21 days. For completeness, functional outcome measures were also recorded along with histology to detect vascular changes in the nerve tissue.

A subsequent study then explored the delivery of ibuprofen sodium and also sulindac sulfide using a PLGA nanofibrous wrap. The wrap option enabled the material to be deployed in a nerve crush model which isolated neuronal regeneration rate from other factors such as pathfinding that can influence recovery in more severe (transection) models.

Ibuprofen-loaded EVA

Immunodetection of neurofilament-positive neurons in transverse sections showed that EVA loaded with 2% ibuprofen sodium increased the number of axons in the distal stump 21 days after transection injury in comparison to EVA with no drug (Figure 8 (d)). Furthermore, the number of axons as a percentage of the proximal stump was higher in the ibuprofen sodium treatment group in comparison to the control group with 160% compared with 105% respectively (Figure 8 (e)). The EVA tubes implanted *in vivo* were harvested and the residual ibuprofen was measured. After re-dissolving the tubes in chloroform and measuring the

remaining ibuprofen using UV-Vis spectrophotometry, it was found that ~ 94.9% ± 0.8 of the drug was released over the 21 days.

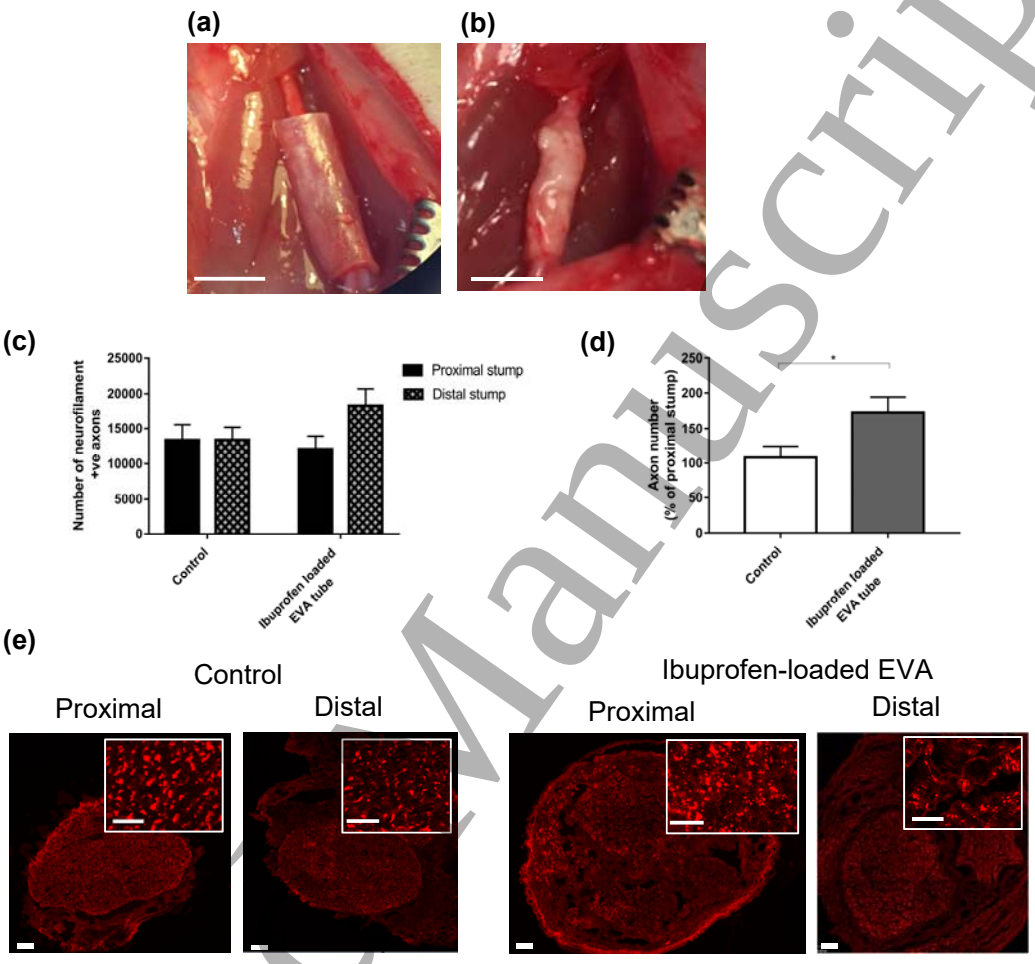

*Figure 8: Axon number in a transection injury model with an implanted ibuprofen-loaded EVA tube. Surgically implanted EVA tubes (a) and harvesting tubes at 21 days post injury (b). Scale bar = 5 mm. Axons were quantified by counting the number of neurofilament-positive cells in the proximal stump and distal stump at 21 days post injury. The number of axons in the distal stump increased in the group with an implanted ibuprofen-loaded EVA tube in comparison to the blank EVA tube (c). Also the number of axons in the distal nerve stump exceeded those in the proximal stump (c). The number of neurofilament-positive axons as a percentage of proximal stump was higher in the ibuprofen treatment group (d). Micrographs are 10 µm transverse sections showing neurofilament positive neurites (e). Scale bar = 100 µm, inset panel = 10 µm. N=6, mean ± SEM for each condition. Two-way ANOVA (c), and two-tailed t-Test (d), *p < 0.05.*

Semi-thin sections (0.5 µm) were taken from the proximal stump (5 mm from injury site) and distal stump (5 and 10 mm from injury site) and stained with toluidine blue to evaluate cellular features of the nerve tissue (Supplementary figure 1). No visual differences were seen between the ibuprofen treated and control group.

Motor and sensory recovery was studied at the 21 day end point using muscle weight, static sciatic index, electrophysiology, and von Frey analysis. Deficiencies were seen in the injured nerves compared to contralateral uninjured nerves with all measures and in all treatment/control groups, indicating that the transection model resulted in a loss of nerve function that persisted at the 21 day time point (Supplementary figure 2).

Vascularisation was examined via immunohistochemical staining of transverse sections for RECA-1. Analysis revealed the presence of blood vessels throughout the injured nerves in both the proximal and distal sections. A higher number and larger blood vessel diameter was observed in the distal stump of the ibuprofen sodium treated group in comparison with the control group. Vasculature in the injured nerves in the ibuprofen-treated group revealed ~25 blood vessels per nerve with a mean diameter of ~18 µm, whereas, the control group presented ~15 blood vessels per nerve with a diameter of ~12 µm (Figure 9).

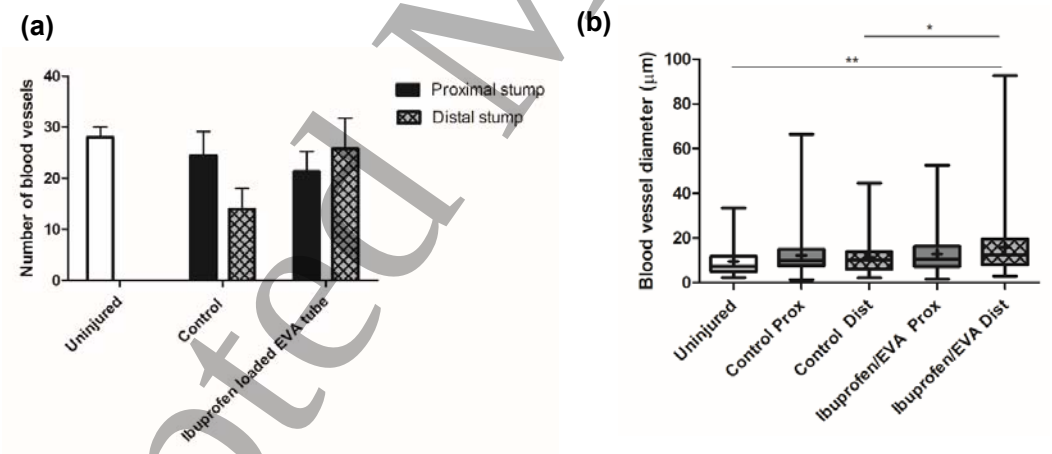

*Figure 9: Quantitative analysis of the number (a) and diameter (b) of blood vessels by RECA-1). N=6, mean ± SEM for each condition, One-way ANOVA with Tukey's post hoc test, *p < 0.05, **p < 0.01. Box plots show the distribution of blood vessel diameter with boxes extending from the max to min, + indicates mean.*

Ibuprofen sodium and sulindac sulfide-loaded PLGA

PLGA nanofibre sheets loaded with ibuprofen sodium or sulindac sulfide were surgically implanted into a rat sciatic nerve as a wrap around a crush injury then assessed over 28 days. The PLGA nanofibres had appropriate handling properties for surgical implantation around the injured nerve (Figure 10 (a), (b)). Transverse sciatic nerve sections were stained to detect

neurofilament immunoreactivity in order to quantify axon numbers. The results demonstrated that both ibuprofen sodium and sulindac sulfide showed a trend towards increased numbers of axons in the distal stump in comparison to the control, however, the differences were not statistically significant (Figure 10 (c-f)).

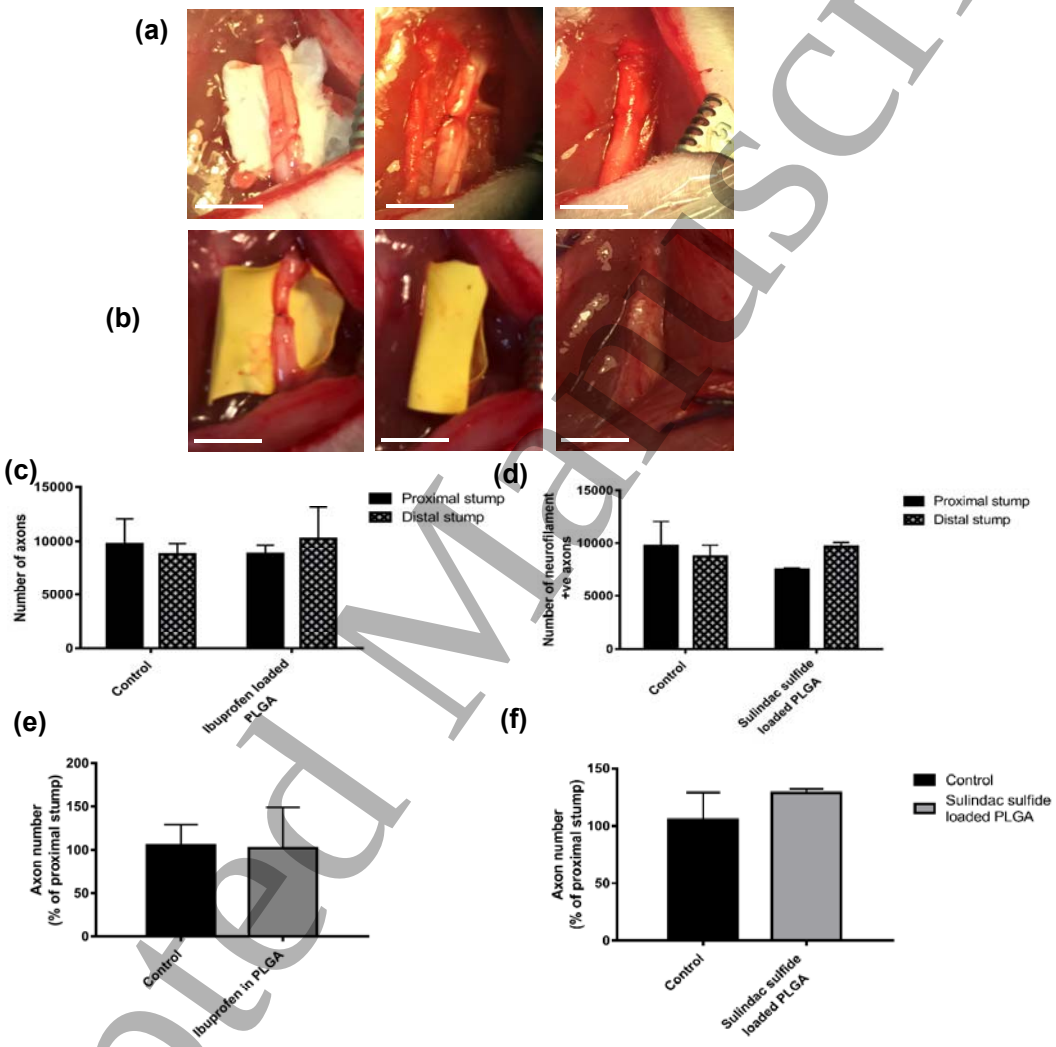

Figure 10: Axon number in a crush injury model with implanted ibuprofen sodium or sulindac sulfide-loaded PLGA nanofibres. Surgically implanted and harvesting at 28 days of ibuprofen-loaded PLGA wraps (a) and sulindac sulfide-loaded PLGA wraps (b). Scale bar = 5 mm. Axons were quantified by counting the number of neurofilament-positive cells in the proximal and distal stumps. The number of axons in the distal stump increased in the groups with implanted ibuprofen sodium (c, d) and sulindac sulfide-loaded (e, f) PLGA nanofibres in comparison to their corresponding control groups at 28 days. N=3 (sulindac sulfide), N=4 (ibuprofen sodium), mean ± SEM for each condition. Two-way ANOVA (c, d), and two-tailed T-Test (e, f), no significance.

Semi-thin sections (0.5 µm) were taken from the proximal stump (5 mm from injury site) and distal stump (5 and 10 mm from injury site) and stained with toluidine blue to evaluate axon myelination. No differences were seen between the two groups (Supplementary figure 3).

Muscle mass and electrophysiology were assessed at the 28 day end point and SSI and von Frey were measured every 2-3 days throughout the experiment. No differences were seen in the threshold response to the von Frey filaments with sulindac sulfide treatment (Figure 11 (b)). However, the threshold response returned to baseline quicker with ibuprofen-loaded PLGA nanofibres with statistically significant improvement at 20 and 22 days post-injury in comparison with the control group (Figure 11 (a)).

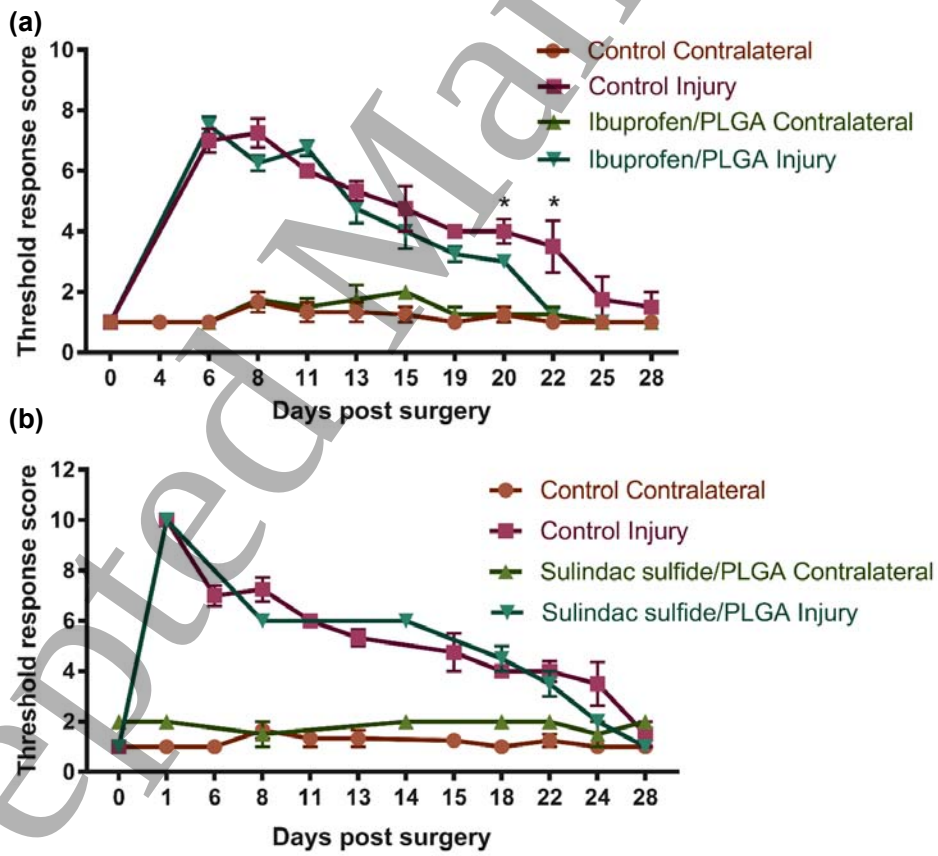

*Figure 11: Von Frey following a crush injury treated with ibuprofen sodium and sulindac sulfide-loaded PLGA nanofibres. The threshold response returned to baseline quicker in the ibuprofen sodium (a) and sulindac sulfide (b) treatment groups in comparison to the control groups after 28 days. N=3 (sulindac sulfide), N=4 (ibuprofen sodium), mean ± SEM, Multiple T-tests between the injured groups at each time point *p<0.05.*

SSI was continuously lower in the ibuprofen sodium treatment group from day 4 with statistical significance seen at days 6 and 8. The SSI also returned to baseline quicker in the ibuprofen sodium treatment group than the control. This occurred by 22 days post-injury with ibuprofen-loaded PLGA nanofibres, but by day 28 in the control group (Figure 12 (a)). Small differences were seen in the sulindac sulfide treatment group in comparison to the control, but improvements between day 1 and 11 post injury can be observed. SSI also returned to baseline quicker in the treatment group that the control group, 25 and 28 days respectively (Figure 12 (b)).

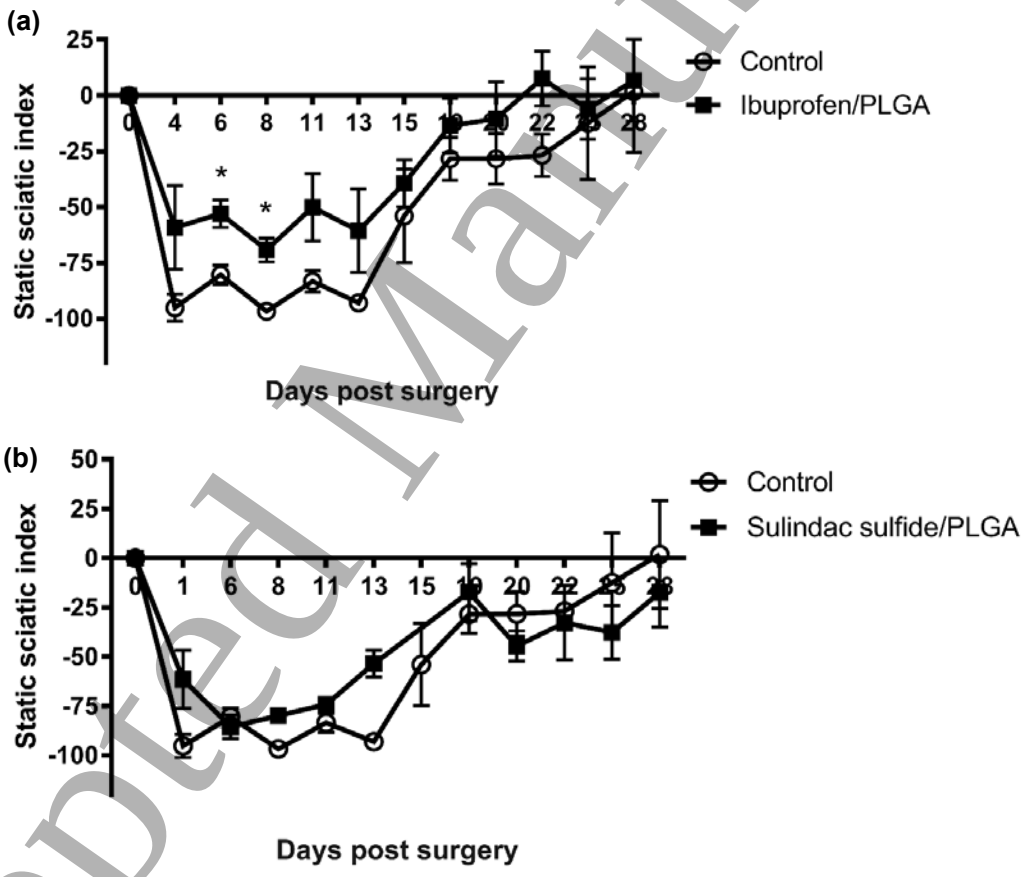

*Figure 12: SSI following a crush injury treated with ibuprofen sodium and sulindac sulfide-loaded PLGA nanofibres. A significant difference in the SSI was seen between the ibuprofen sodium treatment groups and the control (a) but no in the sulindac sulfide (b) treatment group. N=3 (sulindac sulfide) N=4 (ibuprofen sodium), means ± SEM, multiple T-tests, *p<0.05.*

No differences was seen with the gastrocnemius muscle mass with either ibuprofen sodium or sulindac sulfide treatment (data not shown).

Electrophysiology was used to investigate the response of the gastrocnemius muscle to electrical stimulation of the proximal nerve. CMAPs were recorded from the gastrocnemius muscle in the contralateral and injured side in all animals. The CMAP in the ibuprofen sodium treated group was significantly higher than that seen in control animals (Figure 13 (a)). There were small reductions in latency (Figure 13 (c)) and required stimulus intensity (Figure 13 (e)) in the ibuprofen sodium treatment group in comparison with the control group although these were not statistically significant. No difference was observed in the CMAP, latency or the stimulus intensity between sulindac sulfide treatment group and the control (Figure 13 (b, d, and f)).

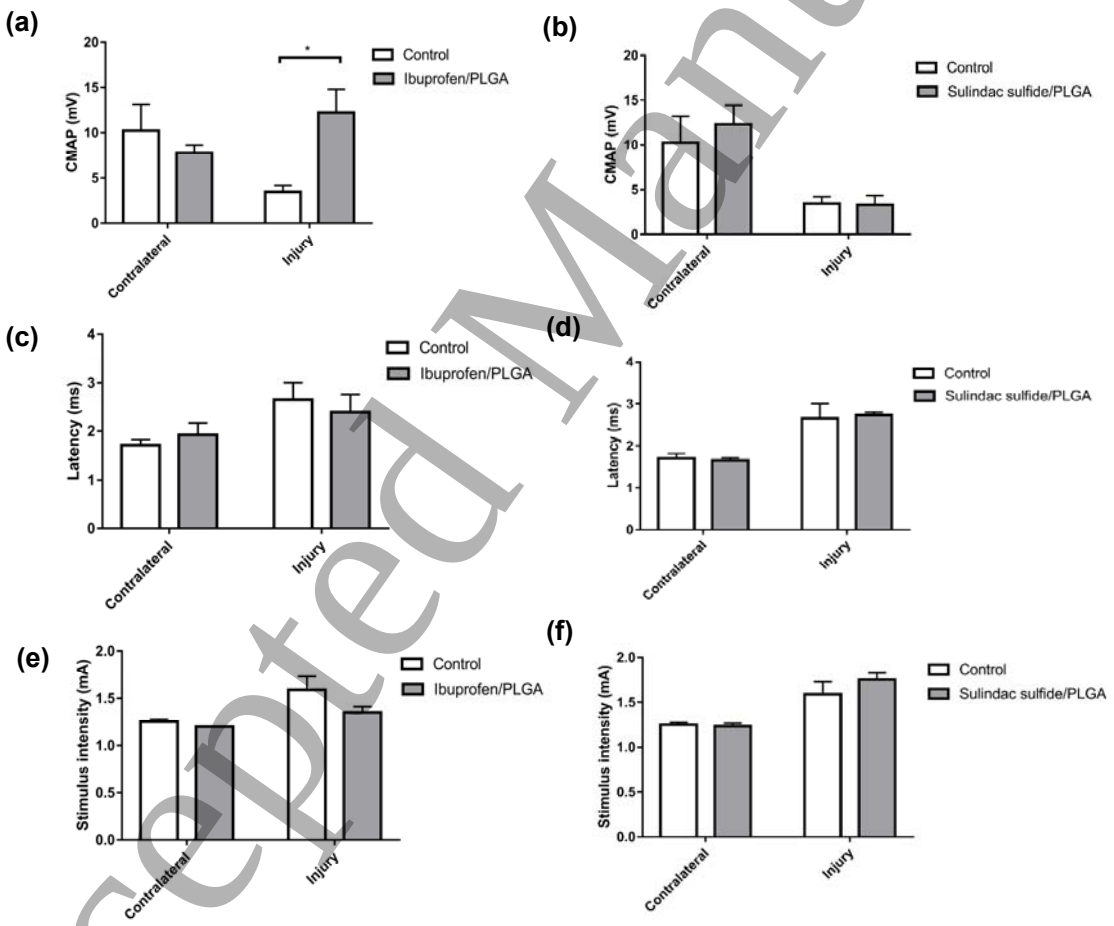

*Figure 13: Electrophysiological evaluation of a crush injury treated with ibuprofen sodium or sulindac sulfide-loaded PLGA nanofibres at 28 days. The CMAP was significantly higher in the treatment group at 28 days following ibuprofen sodium treatment (a) but not with sulindac sulfide treatment (b). No difference was seen in the latency with either drug treatment (c, d). The stimulus intensity was lower in the ibuprofen sodium treatment group in comparison to the control but was not significantly significant (e) and there was no difference seen with sulindac sulfide treatment (f). N=3 (sulindac sulfide), N=4 (ibuprofen sodium), means ± SEM, Two-way ANOVA, *p<0.05.*

Vascularisation analysis demonstrated a higher number of blood vessels in the proximal stump in comparison with the distal stump with both drugs. There was an increase in blood vessel number observed with ibuprofen sodium treatment at 28 days post-injury (Figure 14 (a)). A difference was observed between the two groups with more blood vessels present in the distal stump of the sulindac sulfide treated group in comparison with the control group but this was not statistically significant (Figure 14 (b)). Furthermore, larger blood vessel diameters were found in the sulindac sulfide treatment group (Figure 14 (d)).

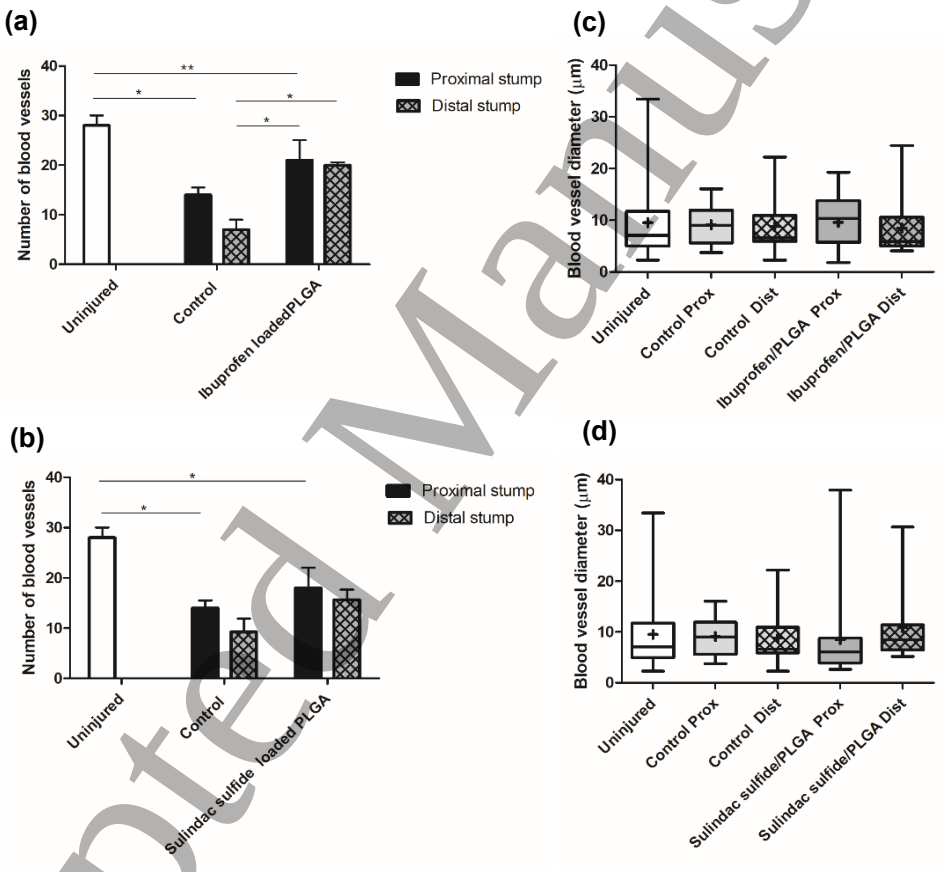

*Figure 14: Vasculature changes following a crush injury treated with ibuprofen sodium and sulindac sulfide-loaded PLGA nanofibres. Quantitative analysis of the number and diameter of blood vessels in ibuprofen-loaded PLGA (a, c) and sulindac sulfide-loaded PLGA (b, d) at 28 days post injury using RECA-1. N=3 (sulindac sulfide), N=4 (ibuprofen sodium), mean ± SEM. One-way ANOVA with Tukey's post-hoc test, *p<0.05, **p<0.01. Box plots show the distribution of blood vessel diameter with boxes extending from the max to min, + indicates mean.*

Discussion

Drug loading into EVA was confirmed using scanning electron microscopy and drug release profiles, with drug release of over 2 weeks. This was the initial target treatment duration, as a previous study had seen positive effects on regeneration following three weeks systemic ibuprofen treatment *(11).* With the EVA membranes there was an initial burst release in the first 4 hours with 60% and 20% of drug released from the membranes and tubes respectively, then within 24 hours this subsided and the release became more constant. This was consistent with a previous study that also observed a burst release of ibuprofen from EVA in the first few hours with 50% of the initial loaded drug released within the 24 hours, then the release subsided after 48 hours with the remainder of the drug released in 10 days *(33)*. The EVA membranes could be successfully manufactured into tubes and it was evident that the geometry of the EVA affected the release rate *in vitro* with the tubes displaying a slower release.

Based on the *in vitro* data showing that EVA tubes could be used as a reproducible material for local delivery of ibuprofen sodium these were tested in a rat sciatic nerve transection model. The primary outcome measure in this case was histological detection of the number of neurites that had grown into the distal stump. The 3 week time period was chosen as this is the treatment duration previously reported in the literature and enabled comparisons to be made *(11, 12)*. Histological analysis of cross sections demonstrated an increase in axon number in the distal stump in the treatment group, which is consistent with previously reported data using osmotic pumps to deliver ibuprofen to transected nerves over 21 days (12). Since the increase in the number of neurites detected in the distal stump of ibuprofen/EVA treated animals was greater than the number in the proximal stump, this indicates that ibuprofen sodium may have been acting to increase sprouting as well as having an effect on accelerating neurite extension.

A previous study that showed functional improvements with systemic ibuprofen treatment in a rat tibial nerve graft model reported similar numbers of axons in ibuprofen treatment and control groups distally at 12 weeks *(11).* Assuming that local delivery of ibuprofen acts

in a similar manner to systemic administration then this increased neurite number in the distal stump at 21 days would be expected to lead to a similar subsequent improvement in functional recovery, perhaps associated with increased maturation and myelination of axons at 12 weeks *(11).* Light microscopy images of the distal stump showed no distinct differences in axon myelination between the control and treatment groups at 21 days. A previous study showed that following a transection injury the mean fibre diameter began to increase between 50 and 150 days, so 21 days may be too early to detect a difference *(34)*.

While the action of ibuprofen on increased regeneration has been attributed to acceleration of neurite elongation as an agonist of PPARγ *(11, 12)*, other mechanisms may contribute, for example the nerve vasculature which is associated with initial Schwann cell guidance and improved regeneration *(35) (36)*. Vascularisation was higher in the ibuprofen sodium treatment group in terms of both number of blood vessels and blood vessel diameter observed here. Little is known about the mechanisms by which drugs modulate nerve regeneration via changes in vascularisation, so this observation is an important consideration and further investigation should explore whether it may be a cause or a consequence of increased neuronal growth.

EVA was a useful and well established biomaterial for initial testing of the hypothesis that local delivery of ibuprofen to nerves could be achieved, but while it has clinical applicability as a drug delivery material in other indications its non-degradability makes it suboptimal for translation to clinical nerve repair applications. For this reason, additional studies were undertaken to develop approaches that could be used to deliver drugs to nerves using degradable materials more suitable for clinical translation.

Ibuprofen-loaded PCL demonstrated burst release of drug in the first four hours (22%), however, only 26% of drug had been released by day 10, which is typical behaviour of a biodegradable material *(37)*. PCL is a commonly used biomaterial and has been used in PNI studies including attempts at drug delivery *(22, 38)* although the rapid initial release of ibuprofen sodium from PCL membranes in this study precluded it being taken forward for *in vivo* testing. Embedding MSN loaded with ibuprofen sodium *(25)* within PCL membranes

improved the release profile, abrogating the initial burst of drug and providing a more controlled release which continued for 14 days. This provides a promising system to be explored further as a drug delivery platform for PNI although challenges associated with achieving robust and reproducible manufacture prevented it from being tested further within this study.

Electrospinning PLGA with ibuprofen sodium resulted in smooth, uniform and bead-free nanofibres with a diameter of ~900 nm. From the results the material and drug were compatible and there appeared to be no strong bonds between the two. The drug release from the PLGA was controlled exhibiting first order kinetics, over 1 week, which is more sustained than results seen in a previous study where electrospun PLGA loaded with 10% ibuprofen exhibited a rapid release over the first 8 hours *(39)*.

As PLGA is biodegradable (~100 days to fully degrade (40)), and the electrospun PLGA formulation used here showed appropriate drug release properties it was taken forward for testing *in vivo*, using a crush model in which recovery of function could be monitored.

Histological analysis demonstrated an increase in axon number in the distal stump in the treatment group at 28 days when treated with both ibuprofen sodium and sulindac-sulfide. Interestingly, with ibuprofen sodium the number of axons in the distal stump exceeded those in the proximal stump in the same animal, indicating increased sprouting as seen following treatment with ibuprofen-loaded EVA tubes.

There are no previous reports exploring the effect of sulindac sulfide for PNI, however, sulindac sulfide was previously shown to inhibit the activity of Rho in a concentration-dependent manner. The direct effect of sulindac sulfide on Rho activation was explored in SY5YAPP, HEK 293 and PC12 cells and levels of active Rho-GTP were reduced in all of the cell lines tested demonstrating that sulindac sulfide inhibits Rho activation *(41)*. Therefore we hypothesised that sulindac sulfide may have a similar effect to ibuprofen sodium on increasing axon growth.

The electrophysiological results, SSI and von Frey analysis all indicated that ibuprofen sodium released from PLGA nanofibres improved functional recovery, however, there was no improvement detected following sulindac sulfide delivery using PLGA nanofibres. These results further support the conclusion that local delivery of ibuprofen sodium using a biomaterial can improve nerve regeneration following injury. Since sulindac sulfide appeared to have little effect in this model, further studies should be conducted to explore whether it would have an effect using a different dose or duration. Interestingly, PLGA-ibuprofen treatment had no effect on the number of blood vessels observed in the distal stump, but the blood vessel diameter was larger in the ibuprofen sodium treatment group in comparison with the control group. A higher number of blood vessels and a larger diameter was seen in the sulindac sulfide treatment group in comparison with the control group.

This study has provided initial insights into using local delivery of NSAIDs such as ibuprofen sodium and sulindac sulfide to promote regeneration in PNI. In future studies more in-depth analysis could be conducted to build a greater understand of the molecular and cellular basis of how these drugs act. Additional quantitative analysis of axon myelination number and size in transverse sections would be a useful indicator of functional success in regeneration *(42)* and other features such as axon sprouting, reconnection and synapse formation could be investigated using longitudinal sections of nerve tissue and retrograde labelling. Furthermore, additional immunostaining could provide insight onto the effect of drug treatment on specific cell types such as Schwann cells or macrophages.

There are several nerve injury animal models used for PNI *(43)*, with an extensive range of outcome measures available to quantify regeneration and recovery of function *(44)*. In this study the nerve transection model was used in the initial experiments where EVA tubes were tested, then the nerve crush model was used to test the use of PLGA nanofibres. Recovery is expected to take longer in a transection injury as there is complete discontinuation of the nerve structure that causes an interface for regenerating axons to navigate, whereas in a crush the nerve tissue architecture is preserved and there is minimal disruption to guidance of

regeneration *(45)*. Outcome measures returned to baseline 28 days following crush injury, which is similar to previous studies *(46, 47).* It would be interesting to use a shorter duration crush injury study to increase the histological detection of differences in regeneration rate caused by the drug treatments. Furthermore, because the treatment durations used here might not provide sufficient time for the distal segments of transected axons to achieve long-distance regeneration, longer end points should also be investigated in future studies. Assessing the effect of local drug release over longer treatment durations would also enable the investigation of any toxicity or other detrimental effects the biomaterials may cause. The materials selected here are already used for drug delivery in other applications so adverse reactions *in vivo* are unlikely, but it will be important to confirm that the solvents and processes used in any future scaled-up production have no detrimental effect on nerve regeneration or drug bioactivity.

The local delivery of a drug to accelerate nerve regeneration has potential application a wide range of nerve injury and disease scenarios and while the present study was limited to testing specific drug/material combinations in transection or crush models it would be advantageous to test the approach in different injury scenarios. Particular indications include gap repair and delayed repair, where the extended duration of muscle denervation reduces the effectiveness of current surgical repair options. Testing whether other NSAIDs and PPARγ agonists can elicit similar beneficial effects as ibuprofen on nerve regeneration will be an important step in understanding the mechanism of action and developing potential new therapies.

References

1. Deumens R, Bozkurt A, Meek MF, Marcus MA, Joosten EA, Weis J, et al. Repairing injured peripheral nerves: Bridging the gap. Prog Neurobiol. 2010;92(3):245-76.
2. Hoke A, Brushart T. Introduction to special issue: Challenges and opportunities for regeneration in the peripheral nervous system. Exp Neurol. 2010;223(1):1-4.
3. Hussain G, Wang J, Rasul A, Anwar H, Qasim M, Zafar S, et al. Current Status of Therapeutic Approaches against Peripheral Nerve Injuries: A Detailed Story from Injury to Recovery. Int J Biol Sci. 2020;16(1):116-34.
4. Manoukian OS, Baker JT, Rudraiah S, Arul MR, Vella AT, Domb AJ, et al. Functional polymeric nerve guidance conduits and drug delivery strategies for peripheral nerve repair and regeneration. J Control Release. 2020;317:78-95.
5. Federici T, Liu JK, Teng Q, Yang J, Boulis NM. A means for targeting therapeutics to peripheral nervous system neurons with axonal damage. Neurosurgery. 2007;60(5):911-8; discussion -8.
6. Kuffler DP. An assessment of current techniques for inducing axon regeneration and neurological recovery following peripheral nerve trauma. Prog Neurobiol. 2014;116:1-12.
7. Bhangra KS, Busuttil F, Phillips JB, Rahim AA. Using Stem Cells to Grow Artificial Tissue for Peripheral Nerve Repair. Stem Cells Int. 2016;2016:7502178.
8. Busuttil F, Rahim AA, Phillips JB. Combining Gene and Stem Cell Therapy for Peripheral Nerve Tissue Engineering. Stem Cells Dev. 2017;26(4):231-8.
9. Chan KM, Gordon T, Zochodne DW, Power HA. Improving peripheral nerve regeneration: from molecular mechanisms to potential therapeutic targets. Exp Neurol. 2014;261:826-35.
10. Bota O, Fodor L. The influence of drugs on peripheral nerve regeneration. Drug Metab Rev. 2019:1-27.
11. Madura T, Tomita K, Terenghi G. Ibuprofen improves functional outcome after axotomy and immediate repair in the peripheral nervous system. J Plast Reconstr Aesthet Surg. 2011;64(12):1641-6.
12. Rayner M, Laranjeira S, Evans R, Shipley R, Healy J, Phillips J. Developing an *in vitro* model to screen drugs for nerve regeneration. Anatomical Record. 2018;In Press.
13. Langert KA, Brey EM. Strategies for Targeted Delivery to the Peripheral Nerve. Front Neurosci. 2018;12:887.
14. Tajdaran K, Chan K, Gordon T, Borschel GH. Matrices, scaffolds, and carriers for protein and molecule delivery in peripheral nerve regeneration. Exp Neurol. 2019;319:112817.
15. Fu Y, Kao WJ. Drug release kinetics and transport mechanisms of non-degradable and degradable polymeric delivery systems. Expert Opin Drug Deliv. 2010;7(4):429-44.
16. Schneider C, Langer R, Loveday D, Hair D. Applications of ethylene vinyl acetate copolymers (EVA) in drug delivery systems. J Control Release. 2017;262:284-95.
17. Zhang W, Gao Y, Zhou Y, Liu J, Zhang L, Long A, et al. Localized and sustained delivery of erythropoietin from PLGA microspheres promotes functional recovery and nerve regeneration in peripheral nerve injury. Biomed Res Int. 2015;2015:478103.
18. Zhang B. Potential use of ethylene vinyl acetate copolymer excipient in oral controlled release application: A literature review. Celanese. 2015:1-10.
19. Neal RA, Tholpady SS, Foley PL, Swami N, Ogle RC, Botchwey EA. Alignment and composition of laminin-polycaprolactone nanofiber blends enhance peripheral nerve regeneration. J Biomed Mater Res A. 2012;100(2):406-23.
20. Sun M, Kingham PJ, Reid AJ, Armstrong SJ, Terenghi G, Downes S. In vitro and in vivo testing of novel ultrathin PCL and PCL/PLA blend films as peripheral nerve conduit. J Biomed Mater Res A. 2010;93(4):1470-81.
21. ClinicalTrials.gov. A Phase I Trial of a Novel Synthetic Polymer Nerve Conduit 'Polynerve' in Participants With Sensory Digital Nerve Injury (UMANC) U.S. National Library of Medicine2016

[updated December, 2017September 2018]. Available from: https://clinicaltrials.gov/ct2/show/NCT02970864.
22. Salmoria GV, Paggi PA, Castro F, Roesler CRM, Moterle D, Kanis LA. Development of PCL/Ibuprofen tube for pripheral nerve regeneration. The Second CIRP Conference on Biomanufacturing2016.
23. Wang Z, Han N, Wang J, Zheng H, Peng J, Kou Y, et al. Improved peripheral nerve regeneration with sustained release nerve growth factor microspheres in small gap tubulization. Am J Transl Res. 2014;6(4):413-21.
24. Giret S, Wong Chi Man M, Carcel C. Mesoporous-Silica-Functionalized Nanoparticles for Drug Delivery. Chemistry. 2015;21(40):13850-65.
25. Zhang H, Li Z, Xu P, Wu R, Wang L, Xiang Y, et al. Synthesis of novel mesoporous silica nanoparticles for loading and release of ibuprofen. J Control Release. 2011;152 Suppl 1:e38-9.
26. Cho CW, Choi JS, Shin SC. Controlled release of pranoprofen from the ethylene-vinyl acetate matrix using plasticizer. Drug Dev Ind Pharm. 2007;33(7):747-53.
27. Mariotti G, Vannozzi L. Fabrication, Characterization, and Properties of Poly (Ethylene-Co-Vinyl Acetate) Composite Thin Films Doped with Piezoelectric Nanofillers. Nanomaterials (Basel). 2019;9(8).
28. Del Angel-Sanchez K, Borbolla-Torres CI, Palacios-Pineda LM, Ulloa-Castillo NA, Elias-Zuniga A. Development, Fabrication, and Characterization of Composite Polycaprolactone Membranes Reinforced with TiO2 Nanoparticles. Polymers (Basel). 2019;11(12).
29. Eren Boncu T, Ozdemir N, Uskudar Guclu A. Electrospinning of linezolid loaded PLGA nanofibers: effect of solvents on its spinnability, drug delivery, mechanical properties, and antibacterial activities. Drug Dev Ind Pharm. 2020;46(1):109-21.
30. Benito C, Davis CM, Gomez-Sanchez JA, Turmaine M, Meijer D, Poli V, et al. STAT3 Controls the Long-Term Survival and Phenotype of Repair Schwann Cells during Nerve Regeneration. J Neurosci. 2017;37(16):4255-69.
31. Bervar M. Video analysis of standing--an alternative footprint analysis to assess functional loss following injury to the rat sciatic nerve. J Neurosci Methods. 2000;102(2):109-16.
32. Schneider CA, Rasband WS, Eliceiri KW. NIH Image to ImageJ: 25 years of image analysis. Nat Methods. 2012;9(7):671-5.
33. Thai QA, Oshiro EM, Tamargo RJ. Inhibition of experimental vasospasm in rats with the periadventitial administration of ibuprofen using controlled-release polymers. Stroke. 1999;30(1):140-7.
34. Ikeda M, Oka Y. The relationship between nerve conduction velocity and fiber morphology during peripheral nerve regeneration. Brain Behav. 2012;2(4):382-90.
35. Cattin AL, Burden JJ, Van Emmenis L, Mackenzie FE, Hoving JJ, Garcia Calavia N, et al. Macrophage-Induced Blood Vessels Guide Schwann Cell-Mediated Regeneration of Peripheral Nerves. Cell. 2015;162(5):1127-39.
36. Best TJ, Mackinnon SE. Peripheral nerve revascularization: a current literature review. J Reconstr Microsurg. 1994;10(3):193-204.
37. Yang WW, Pierstorff E. Reservoir-based polymer drug delivery systems. J Lab Autom. 2012;17(1):50-8.
38. Allen C, Eisenberg A, Mrsic J, Maysinger D. PCL-b-PEO micelles as a delivery vehicle for FK506: assessment of a functional recovery of crushed peripheral nerve. Drug Deliv. 2000;7(3):139-45.
39. Canton I, McKean R, Charnley M, Blackwood KA, Fiorica C, Ryan AJ, et al. Development of an Ibuprofen-releasing biodegradable PLA/PGA electrospun scaffold for tissue regeneration. Biotechnol Bioeng. 2010;105(2):396-408.
40. Riggin CN, Qu F, Kim DH, Huegel J, Steinberg DR, Kuntz AF, et al. Electrospun PLGA Nanofiber Scaffolds Release Ibuprofen Faster and Degrade Slower After In Vivo Implantation. Ann Biomed Eng. 2017;45(10):2348-59.

41. Zhou Y, Su Y, Li B, Liu F, Ryder JW, Wu X, et al. Nonsteroidal anti-inflammatory drugs can lower amyloidogenic Abeta42 by inhibiting Rho. Science. 2003;302(5648):1215-7.
42. Ronchi G, Raimondo S, Geuna S, Gambarotta G. New insights on the standardization of peripheral nerve regeneration quantitative analysis. Neural Regen Res. 2015;10(5):707-9.
43. Angius D, Wang H, Spinner RJ, Gutierrez-Cotto Y, Yaszemski MJ, Windebank AJ. A systematic review of animal models used to study nerve regeneration in tissue-engineered scaffolds. Biomaterials. 2012;33(32):8034-9.
44. Rayner MLD, Brown HL, Wilcox M, Phillips JB, Quick TJ. Quantifying regeneration in patients following peripheral nerve injury. J Plast Reconstr Aesthet Surg. 2020;73(2):201-8.
45. Tos P, Ronchi G, Papalia I, Sallen V, Legagneux J, Geuna S, et al. Chapter 4: Methods and protocols in peripheral nerve regeneration experimental research: part I-experimental models. Int Rev Neurobiol. 2009;87:47-79.
46. Pavic R, Pavic ML, Tvrdeic A, Tot OK, Heffer M. Rat sciatic nerve crush injury and recovery tracked by plantar test and immunohistochemistry analysis. Coll Antropol. 2011;35 Suppl 1:93-100.
47. Ramli D, Aziz I, Mohamad M, Abdulahi D, Sanusi J. The Changes in Rats with Sciatic Nerve Crush Injury Supplemented with Evening Primrose Oil: Behavioural, Morphologic, and Morphometric Analysis. Evid Based Complement Alternat Med. 2017;2017:3476407.